Anal. Chem. **2006,** *78,* 7499−7503

1D and 2D Temperature Imaging with a Fluorescent Ruthenium Complex

Oscar Filevich and Roberto Etchenique*

Departamento de Química Inorgánica, Analítica y Química Física, INQUIMAE, Facultad de Ciencias Exactas y Naturales, Universidad de Buenos Aires, Ciudad Universitaria Pabellon 2 Piso 3. C1428EHA, Buenos Aires, Argentina

Temperature imaging based on the fluorescence of the complex $[Ru(bpy)_3]^{2+}$ is described. The method allows precise temperature measurement on unidimensional flow injection reactors and bidimensional measurement on dishes for biological and biochemical assays. The fluorescence dependence on temperature is linear, achieving a resolution of 0.05 K with a simple two-point calibration. The large Stokes shift of $[Ru(bpy)_3]^{2+}$ makes it easy to use a simple CCD camera without special filters. Large or small area fields can be achieved by changing the optics of the camera. High spatial resolution is possible by using any fluorescence microscope.

Temperature plays a key role in most chemical reactions, and therefore, its precise measurement has become an important issue in almost all studies in chemistry. While bulk systems can be thermostated, and their temperature can be measured by means of standard techniques (i.e., normal-sized thermometers, thermocouples, NTC thermistors, and similar devices), very small systems like reactors used in continuous systems (FIA, SIA, etc.) or microfluidics need a different approach, and new techniques have been devised to control and measure their temperature. The behavior of biological systems often depends very acutely on temperature changes,[1] and in these cases, temperature measurement must be done very accurately to ensure repeatable results. In the case of cell culture studies, the temperature not only has to be constant in time but also in space, as slight temperature variations can cause different behavior in cells under different conditions.

While temperature measurement can be performed by means of many methods, such as UV−visible absorption,[2] near-IR spectroscopy,[3] conductivity,[4] and NMR,[5] fluorescence spectroscopy imaging seems to be the best technique because of its high throughput, capable of measuring temperatures with good precision in thousands or millions of points simultaneously and at very high rates.

The fluorescence of several dyes presents a strong dependence on temperature,[6,7] and this property can be used to image temperature with good results.[8] Cadmium selenide quantum dots[9−11] and inorganic complexes[12−14] have also used in temperature imaging. Unfortunately, the emission dependence on temperature is usually nonlinear and this fact makes the data analysis difficult and increases the possibility of introducing large systematic errors in poorly calibrated systems.

In this work, we present a temperature imaging system using the $[Ru(bpy)_3]^{2+}$ complex and a camera with a CCD sensor. We show that the calibration of this system is very simple, due to the linearity of its response. We apply the method to a standard cell culture Petri dish in a standalone thermostatic chamber for time lapse videomicroscopy and to a FIA reactor coiled as a spiral.

EXPERIMENTAL SECTION

Chemicals and Materials. All chemicals were purchased from Sigma-Aldrich Chemicals. All solutions were degassed with N_2 prior to their use. Polyethylene tubing for FIA measurements of 0.86-mm inside diameter was purchased from A-M Systems (Catalog No. 802200).

Calibration and Imaging. Measurements of the $[Ru(bpy)_3]^{2+}$ fluorescence temperature dependence were performed on a fiber-optic Ocean Optics spectrofluorometer, using a 470-nm blue LED as excitation source. Temperature measurements inside the cuvette were done by means of a calibrated NTC thermistor immersed in the complex solution. The entire system was heated with a hot air flow, at a slow rate to prevent nonthermalization. Images of the fluorescence of aqueous solutions of $[Ru(bpy)_3]^{2+}$ were taken with an 8 Mpixel Canon Rebel XT digital camera, using software based on Canon SDK 8.3 control routines. A high-power LED at 470 nm (Luxeon III, Blue, Lumileds) was used as excitation source, and the frames were taken through an 550-nm gelatin low-

* Corresponding author. E-mail: rober@qi.fcen.uba.ar.

(1) Price, P. B.; Sowers, T. *Proc. Natl. Acad. Sci. U.S.A.* **2004**, *101*, 4631−4636.
(2) Watzig, H. *Chromatographia* **1992**, *33*, 445−448.
(3) Otal, E. H.; Iñón, F. A.; Andrade, F. J. *Applied Spectrosc.* **2003**, *57*, 661−666.
(4) Tallarek, U.; Rapp, E.; Scheenen, T.; Bayer, E.; Van As, H. *Anal. Chem.* **2000**, *72*, 2292−2301.
(5) Lacey, M. E.; Webb, A. G.; Sweedler, J. V. *Anal. Chem.* **2000**, *72*, 4991−4998.
(6) Sakakibara, J.; Hishida, K.; Maeda, M. *Exp. Fluids* **1993**, *16*, 82−96.
(7) Sakakibara, J.; Adrian, R. J. *Exp. Fluids* **1999**, *26*, 7−15.
(8) Ross, D.; Gaitan, M.; Locascio, L. E. *Anal. Chem.* **2001**, *73*, 4117−4123.
(9) Walker, G. W.; Sundar, V. C.; Rudzinski, C. M.; Wun, A. W.; Bawendi, M. G.; Nocera, D. G. *Appl. Phys. Lett.* **2003**, *83*, 3555−3557.
(10) Mao, H.; Yang, T.; Cremer, P. S. J. *Am. Chem. Soc.* **2002**, *124*, 4432−4435.
(11) Biju, V.; Makita, Y.; Sonoda, A.; Yokoyama, H.; Baba, Y.; Ishikawa, M. *J. Phys. Chem. B* **2005**, *109*, 13899−13905.
(12) Durham, B.; Caspar, J. V.; Nagle, J. K.; Meyer, T. J. *J. Am. Chem Soc.* **1982**, *104*, 4803−4810.
(13) Kolodner, P.; Tyson, A. *Appl. Phys. Lett.* **1982**, *40*, 782−784.
(14) Zohar, O.; Ikeda, M.; Shinagawa, H.; Inoue, H.; Nakamura, H.; Elmaum, D.; Alkon, D. L.; Yoshioka, T. *Biophys. J.* **1998**, *74*, 82−89.

10.1021/ac061382f CCC: $33.50
Published on Web 10/05/2006

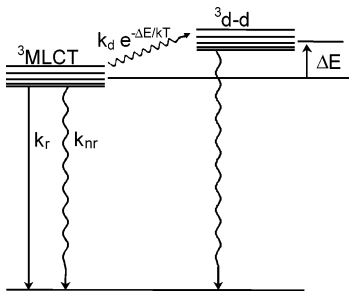

Figure 1. Scheme of the electronic states of $[Ru(bpy)_3]^{2+}$ complex.

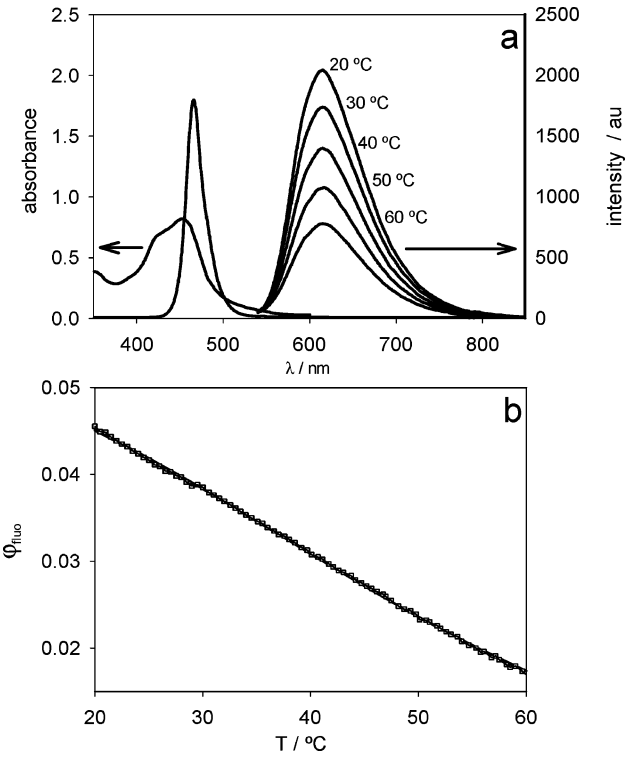

Figure 2. (a) Left: typical absorbance of aqueous $[Ru(bpy)_3]Cl_2$. Right: LED excitation and emission of an aqueous 10^{-5} M solution of $[Ru(bpy)_3]Cl_2$ between 20 and 60 °C. Note the large Stokes shift. (b) Squares: quantum yield of fluorescence of the solution of (a) versus temperature. Solid line: plot of eq 1 with the following parameters, $k_r = 6.8 \times 10^4\ s^{-1}$, $k_{nr} = 1.2 \times 10^6\ s^{-1}$, $k_d = 1.1 \times 10^{13}\ s^{-1}$, and $\Delta E = 3518\ cm^{-1}$.

pass orange filter, to minimize the incidence of blue light reflections in the measurements. The red channel of the 12-bit RAW digital images was preprocessed using IRIS software and then further processed with ImageJ.

The FIA reactor was made by coiling a polyethylene tubing between the inner side of a 250-mL Corning culture flask and an aluminum piece. The spiral tubing was wound as a double spiral, leaving an empty tube in between two consecutive turns in order to minimize the heat conduction through their walls. The bottle was filled with water at the required temperature and was stirred with a magnetic stirrer. The flow of the fluorescent solution was kept by suction and thermalized in a water bath prior to its entry to the reactor.

2D fluorescent screens for temperature imaging were made by encapsulating ~50 μL of a $[Ru(bpy)_3]Cl_2$ solution between two 24 × 24 mm, 0.20-mm-thick cover glasses, using a Parafilm

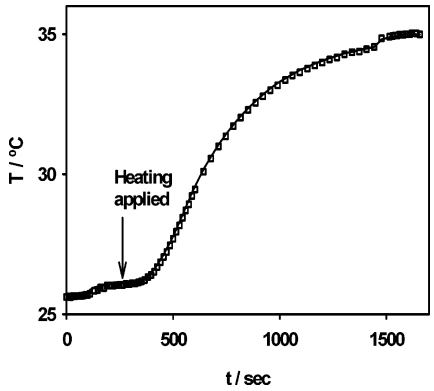

Figure 3. Temperature changes during heating of a Petri dish. Solid line: measured with a calibrated thermistor. Squares: measured with a fluorescent screen filled with a $[Ru(bpy)_3]Cl_2$ solution.

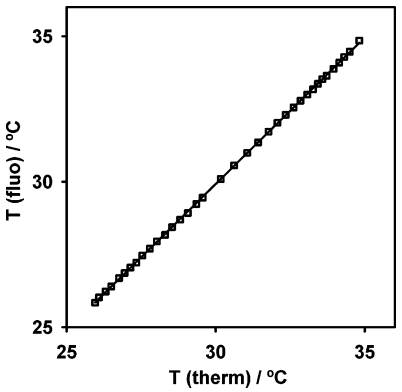

Figure 4. Squares: temperature data taken with the fluorescent screen in a zone of 40 × 40 pixels vs the temperature measured with a thermistor at the same area. Solid line: linear fitting of the data.

separator. After sealing the Parafilm to the coverslips at 80 °C for a few seconds, the complex solution was filled using a 20-μL pipet, and the ends were then sealed with varnish to prevent leakage. The screen was left for 2 h at room temperature until its seal was dry and then used several times without additional care.

The thermostated cell culture chamber consists of an aluminum block, which is heated at its corners by four 33 Ω, 1-W resistors embedded into the block. Body temperature is measured with an LM35 integrated sensor and kept constant at ~37 °C with an operational amplifier circuit with negative feedback (see Supporting Information).

RESULTS AND DISCUSSION

Figure 1 shows a simplified scheme of the electronic states of $[Ru(bpy)_3]^{2+}$ complex.[15] In this model, the original excited state ^{1}MLCT has already relaxed to the ^{3}MLCT, which can decay through emission with rate k_r or through a nonradiative path with rate k_{nr}. It also can cross to the ^{3}d−d state with rate $k_d \exp(-\Delta E/kT)$ and further decay to the ground state. While k_r and k_{nr} are independent of the temperature, the cross from the ^{3}MLCT state to the^{3}d−d is activated, and therefore, k_d and ΔE determine the emision dependence on temperature. In the absence of other processes, and considering that the returning

(15) Van Houten, J. and Watts, R. J. *J. Am. Chem. Soc.* **1976**, *98*, 4853−4858.

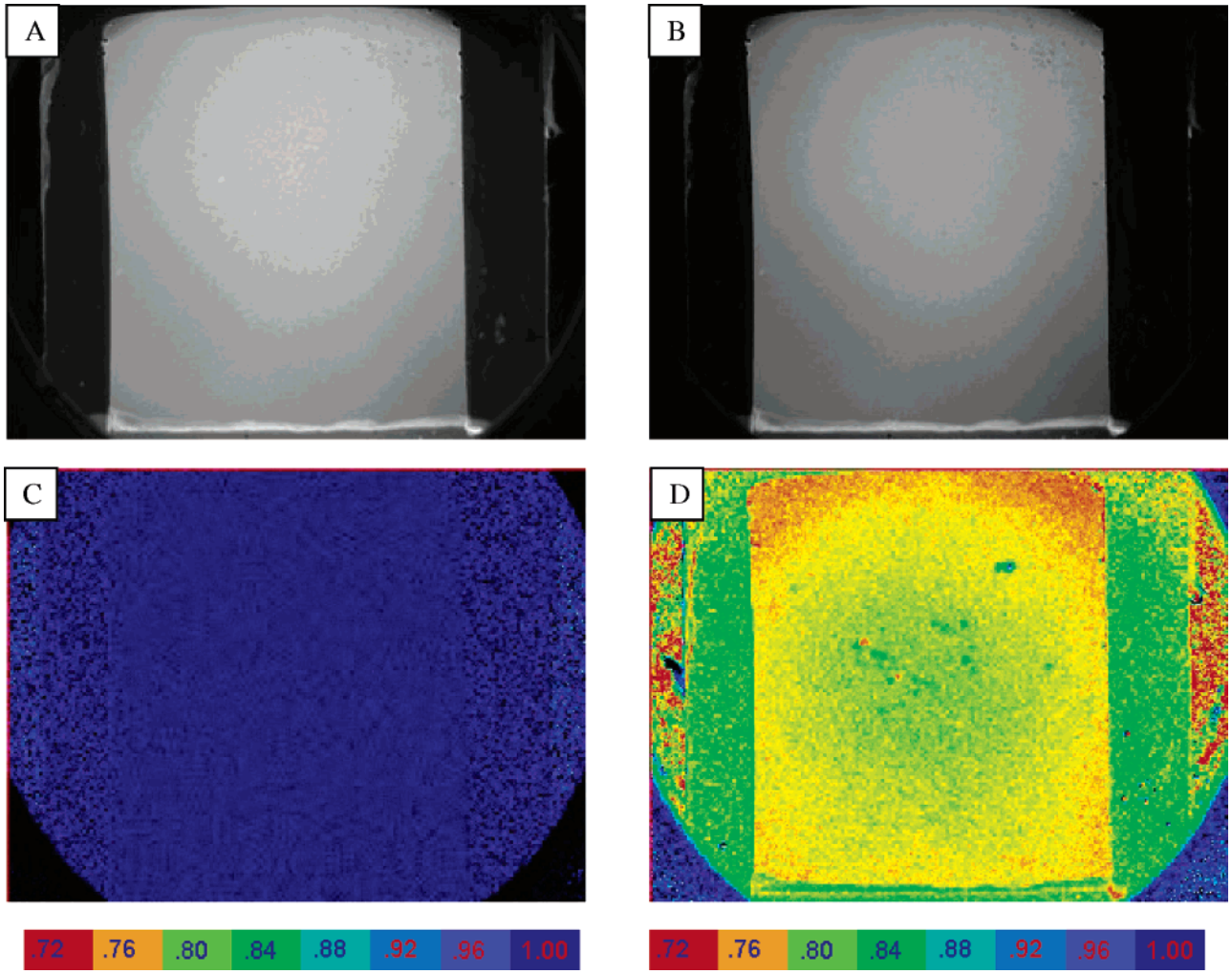

Figure 5. Fluorescence images of a rectangular 22 × 18 mm plate filled with 10 mM $[Ru(bpy)_3]Cl_2$, immersed in water inside a Petri dish. (A) Raw image of the plate at 25 °C. (B) Raw image during heating. (C) False color image of frame A normalized as explained in the text. (D) False color of normalized frame B (note the relative fluorescence changes due to the temperature gradients during the heating). The color scale shows the relative fluorescence intensity. (Values out of the central rectangular screen are not related to temperature.)

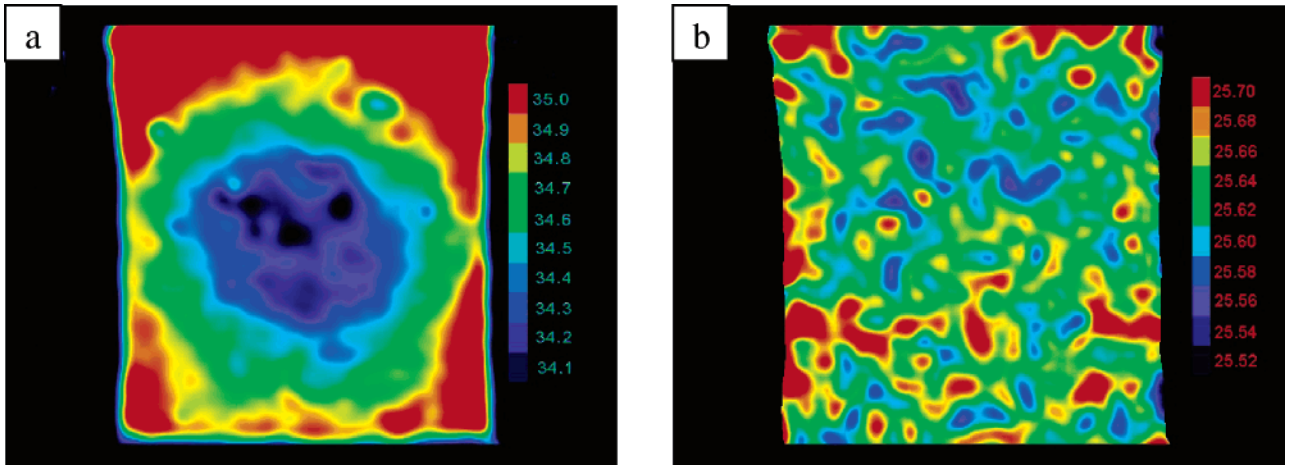

Figure 6. Temperature images of a 22 × 18 mm plate filled with 10 mM $[Ru(bpy)_3]Cl_2$, immersed in water inside a Petri dish. (a) Plate during heating, showing a temperature gradient of ~1 °C. (b) Plate in a thermalized dish. The total span of temperatures corresponds to 0.18 °C. Color scale is *T* in Celsius.

path to the ground state is fast enough, the quantum yield of emission is

$$\phi_r = k_r/[k_r + k_{nr} + k_d \exp(-\Delta E/kT)] \quad (1)$$

The fluorescence of a solution of $[Ru(bpy)_3]^{2+}$ at different temperatures is depicted in Figure 2a. The excitation LED spectrum around 470 nm and the emission show almost no overlap due to the large Stokes shift. A typical absorbance

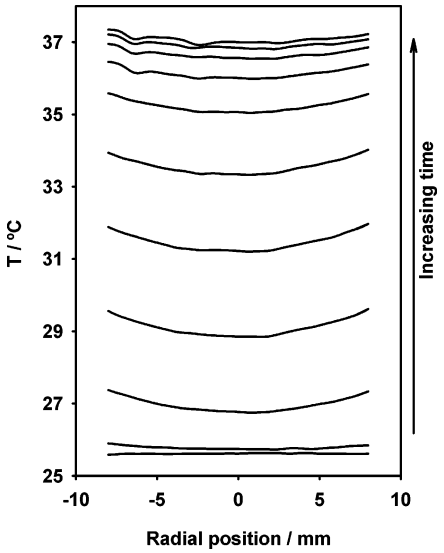

Figure 7. Temperature profiles of a Petri dish measured with a $[Ru(bpy)_3]Cl_2$ screen at different times during heating in a thermostatic cell culture chamber.

spectrum of the complex can be seen at the left for comparison.

Figure 2b shows the quantum yield of fluorescence calculated from the same data. The solid line is the best fit of the parameters of eq 1. It is noteworthy that even though the general dependence is rather complex, the data lay on a well-behaved straight line. This property makes this system very convenient for temperature measurements in the 20−60 °C range.

As the usual working conditions when using an imaging device often include poor excitation light distribution, reflections, etc., a test for robustness was done. We made a simple screen that consists of two cover glasses separated by a Parafilm foil (see Experimental Section), which was filled with 40−60 μL of a 10 mM solution of $[Ru(bpy)_3]Cl_2$. The screen was immersed into a plastic 3.5-cm Petri dish, which was filled with 2 mL of distilled water, and this dish was heated using the thermostated cell culture chamber. A calibrated NTC thermistor was fixed from the top, with its sensor body at 0.5 mm of the screen, totally immersed in the water. The temperature was recorded with the thermistor every 1 s, while the fluorescence images were taken at a rate of 1 frame every 10−30 s.

To ensure that the temperature is the same in all of the dish, stirring is possible with a small magnetic bar. Figure 3 shows the temporal plot of the temperatures measured with the thermistor and the temperature indicated by the fluorescent plate in an area of 40 × 40 pixels that corresponds to the location where the thermistor was placed.

During the first and last 100 s, the measurements were taken while stirring, in order to homogenize the temperature in all the screen. Calibration of the images was done with a simple procedure of two points, taken as the average of five frames each during the stirring periods. (The calibration procedure is detailed in the discussion of Figure 5.) The heating was turned on at 230 s and was kept until the end of the experiment without stirring, as usual.

Figure 4 shows the comparison between the temperature measurements done with the thermistor and the fluorescent plate for the experiment on Figure 3. The high linearity was also confirmed in other experiments from 15 to 65 °C. No hysteresis was observed during repeated cycles of heating−cooling, in agreement with the widely known stability of this ruthenium complex.

During heating, the temperature gradient of the water in the petri dish can be obtained using the imaging procedure. Figure 5 shows a typical procedure by which the temperature plate is imaged using the fluorescent screen, from the initial images to the final results in degrees Celsius.

Several images taken at a known temperature T_1 (usually 25 °C) are averaged to reduce noise. Care must be taken to ensure that the temperature is the same all across the plate. All the other images are normalized to this calibration frame. By this procedure,

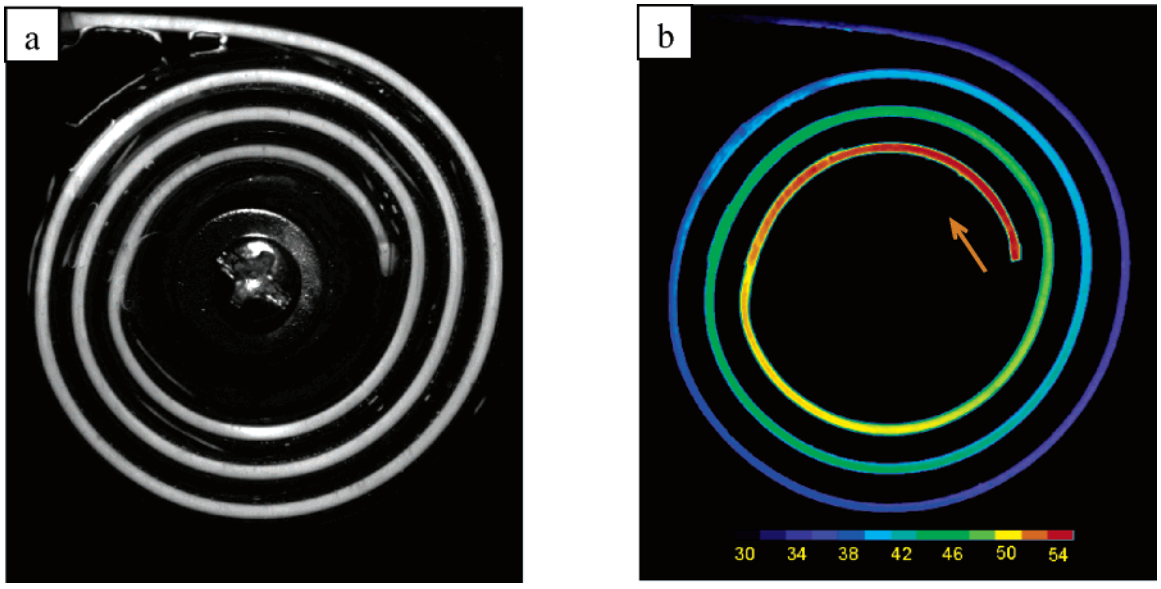

Figure 8. Images of a FIA reactor. A solution of $[Ru(bpy)_3]Cl_2$ enters from the center of the spiral at 55 °C. The spiral is immersed in a cooling bath at 23 °C. (a) Raw image of the reactor. (b) False color temperature image showing the cooling process. Color scale shows temperature in Celsius.

the error due to irregularities on the excitation light distribution is limited to a minimum. The obtained relative frames will have values above 1 for pixels having temperature $T_{pix} < T_1$ and values under 1 for $T_{pix} > T_1$.

A second calibration point can be taken by having a second set of frames at a different temperature T_2. In this case, a slope (m) and intercept (b) for a first-order fitting can be calculated, being

$$m = (T_2 - T_1)/[\text{frame}(T_2) - \text{frame}(T_1)]$$

$$b = T_1 - m \times \text{frame}(T_1)$$

It is possible to know the spatial and temporal changes of temperature by measuring the temperature maps at several times of an experiment. Figure 7 shows the spatial temperature plots taken at regular times during the heating procedure of a Petri dish. The gradient increases to more than 1.2 °C during the heating time and diminishes to less than 0.3 °C when thermostatic control is reached.

The estimation of the measurement error was performed through statistical analysis of the image at a given position. A typical histogram of a 1-mm-diameter circle of the image, containing 436 pixels and with a average value of 25.56 °C presents absolute maximum and minimum pixels of 25.59 and 25.54 °C, respectively, and a standard deviation $\sigma = 0.011$ °C. Therefore, two temperature values with a difference of 0.05 °C can be unambiguously discerned.

The measurement of temperature inside a FIA reactor is depicted in Figure 8. In this case, the imaged object is a 60-cm polyethylene tubing with a 1 mM $[Ru(bpy)_3]Cl_2$ solution flowing through it. The tube is coiled in a spiral, to minimize the needed imaged area, and immersed in 200 mL of water at 25 °C.

Figure 8a shows the raw image of the FIA reactor once achieved stationary state at a constant flow of 60 μL/s. Despite the big differences in illumination and the apparent reflections, a good image of the temperature at any point can be obtained. Figure 9 depicts the plot of the temperature along a line on the spiral reactor. It is important to remark that these data would be almost impossible to obtain by using any kind of discrete temperature sensors. The temperature measured along the tube show the typical exponential behavior, and the parameter k, related to the heat-transfer resistance of the tubing, can be obtained.

In all the presented measurements, the solutions were degassed. In the case of the coverslip screens, the screens were used for many days without noticeable change. It is known that O_2 reduces the emission quantum efficiency of $[Ru(bpy)_3]^{2+}$ by quenching the MLCT state.[16] However, temperature measurements with solutions prepared in presence of air (~20% O_2) gave the same results than those made with degassed solutions. In this case, the slopes of emission versus temperature are lower, and therefore, the images present higher noise, but the relationship between the relative fluorescence to the temperature is still linear.

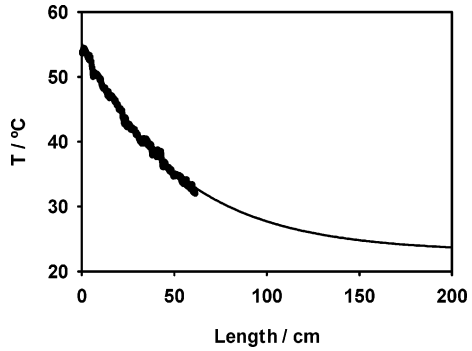

Figure 9. Dark line: plot of the temperature along a line inside the tube in the spiral FIA reactor showed in Figure 8. Light line: best fit of the equation $T = A \exp(-kx) + 23$, with $A = 32.1$ °C and $k = 52.1$ cm^{-1}.

CONCLUSIONS

The method for temperature imaging that we have presented here, based on the fluorescence of the complex $[Ru(bpy)_3]^{2+}$, shows important advantages over other methods. The linear dependence of the emission intensity on the temperature allows the use of a simple two-point calibration, with minimal error. An uncertainty as low as 0.05 °C can be easily achieved. Even a single-point calibration can be used, but large systematic errors can arise in the cases where this point is far from the measurement range. The method can be used in macro- and microscale, and determinations of temperature of small channels can also be obtained. The use of $[Ru(bpy)_3]^{2+}$ emission to determine temperatures in FIA reactors is very easy, and the concentrations can be reduced using higher excitation power or longer exposures.

ACKNOWLEDGMENT

This work was done with the financial support of ANPCyT, UBACyT, and CONICET. R.E. is a member of CONICET.

SUPPORTING INFORMATION AVAILABLE

Stacks of images of time-dependent experiments. This material is available free of charge via the Internet at http://pubs.acs.org.

Received for review July 27, 2006. Accepted August 30, 2006.

AC061382F

(16) Bensasson, R.; Salet, C. and Balzani, V. *J. Am. Chem. Soc.* **1976**, *98*, 3272−3273.